DTU Library

Supersonic acoustic intensity with statistically optimized near-field acoustic holography

Fernandez Grande, Efren; Jacobsen, Finn

[Link back to DTU Orbit](#)

Supersonic acoustic intensity with statistically optimized near-field acoustic holography

Efren Fernandez-Grande[1], Finn Jacobsen[2]

[1] Acoustic Technology. B. 352, Department of Electrical Engineering

DTU (Technical University of Denmark). 2800 Lyngby, Copenhagen, Denmark.

ABSTRACT

The concept of supersonic acoustic intensity was introduced some years ago for estimating the fraction of the flow of energy radiated by a source that propagates to the far field. It differs from the usual (active) intensity by excluding the near-field energy resulting from evanescent waves and circulating energy in the near-field of the source. This quantity is of concern because it makes it possible to identify the regions of a source that contribute to the far field radiation, which is often the ultimate concern in noise control. Therefore, this is a very useful analysis tool complementary to the information provided by the near-field acoustic holography technique. This study proposes a version of the supersonic acoustic intensity applied to statistically optimized near-field acoustic holography (SONAH). The theory, numerical results and an experimental study are presented. The possibility of using particle velocity measurements instead of conventional pressure measurements is examined. The study indicates that the calculation of the supersonic intensity based on measurement of the particle velocity is more accurate than the one based on sound pressure measurements. It also indicates that the method based on SONAH is somewhat more accurate than the existing methodology based on Fourier transform processing.

Keywords: Near-Field Acoustic Holography, NAH, Sound Radiation, Sound Intensity.

1. INTRODUCTION

In noise control and many areas of acoustics, the far field radiation of sources is frequently the ultimate quantity of concern, because it is typically this quantity that is perceived by a potential observer. Therefore, it is often important to identify the regions of a source that contribute to the far field output. This is precisely the aim of the method proposed in the present paper.

Wave bearing structures generally have strong near-field components, namely evanescent waves that decay exponentially and do not transport energy to the far field. An evanescent wave in isolation does not contribute to the active sound intensity because its sound pressure and particle velocity are in quadrature. Nevertheless, in the near-field of vibrating structures, the evanescent waves and propagating waves interact with each other, giving rise to regions of circulatory energy flow [1]. In other words, there is a circulation of active sound intensity flowing from one region of the source into an adjacent one.

In near-field techniques, where measurements take place in the near-field of the source or directly on its surface, this circulatory energy flow makes it difficult to immediately identify the regions that radiate efficiently into the far field and contribute to its net power output. This is for instance the case

---

[1] efg@elektro.dtu.dk

[2] fja@elektro.dtu.dk

in near-field acoustic holography (NAH) [2-3], which is a powerful source identification technique that characterizes completely the sound field radiated by a source, in principle with "unlimited" spatial resolution, making it possible to reconstruct the sound pressure, particle velocity vector, and sound intensity based on near-field acoustic measurements.

Williams [4-5] proposed the useful concept of "supersonic acoustic intensity" for identifying and characterizing the regions of a source that radiate into the far field. The method is based on NAH and the wavenumber space processing of the sound field. Its fundamental principle is to filter out the evanescent waves in the near-field of the source and estimate the active sound intensity based exclusively on the propagating waves. Hence only the efficient radiation of the source is taken into account. So far, the calculation of the supersonic acoustic intensity has only been formulated on the basis of Fourier based NAH.

The authors are inclined to think that the term "supersonic acoustic intensity" can be somewhat confusing, since it might lead to the misunderstanding that the energy in the sound field travels with supersonic speed. Therefore, in the present paper the alternative term "effective sound intensity" has been introduced. However, the notation established in refs. [4-5] is maintained.

Statistically optimized near-field acoustic holography [6-7], most frequently referred to as SONAH, is a holographic method that has the outstanding advantage of operating directly in the spatial domain, avoiding some of the errors associated with the discrete Fourier transformation. This makes the method very useful for the holographic reconstruction of sound fields and patch-NAH.

The aim of this paper is to extend the concept of effective sound intensity or supersonic intensity to SONAH. Because this method relies on an elementary wave decomposition, the evanescent waves can be separated from the propagating ones without Fourier transforming the sound field explicitly. The paper gives the theoretical background, and studies several examples. It also considers the reconstruction based on measurement of the particle velocity instead of sound pressure.

2. THEORY

Statistically optimized near-field acoustic holography (SONAH) is based on an elementary plane wave expansion of the acoustic field. Let the plane wave functions be

$$\psi(\mathbf{r}) = e^{-j(k_x x + k_y y + k_z(z - z^+))} ,$$
(1)

where z^+ is the so called virtual source plane, where the elementary waves are scaled [6]. The wavenumber in the z direction, k_z, depends on k, k_x and k_y as:

$$k_z = \begin{cases} \sqrt{k^2 - (k_x^2 + k_y^2)} & \text{if } k^2 \geq k_x^2 + k_y^2 \\ -j\sqrt{(k_x^2 + k_y^2) - k^2} & \text{if } k^2 < k_x^2 + k_y^2 . \end{cases}$$
(2)

This shows that the plane waves are both propagating and evanescent. In SONAH, the pressure in the measurement plane is decomposed as:

$$\mathbf{p}(\mathbf{r}_h) = \begin{bmatrix} \psi_1(\mathbf{r_1}) & \psi_2(\mathbf{r_1}) & \cdots & \psi_n(\mathbf{r_1}) \\ \vdots & \vdots & & \vdots \\ \psi_1(\mathbf{r_m}) & \psi_2(\mathbf{r_m}) & \cdots & \psi_n(\mathbf{r_m}) \end{bmatrix} \begin{bmatrix} c_1 \\ c_2 \\ \vdots \\ c_n \end{bmatrix} = \mathbf{B}\mathbf{c} ,$$
(3)

where $\mathbf{p}(\mathbf{r}_h)$ is a column vector with the measured pressure, $\mathbf{B}$ is a matrix containing the elementary wave functions and $\mathbf{c}$ is the coefficient vector. On the basis of this elementary wave expansion, the pressure in the reconstruction plane is expressed as

$$\mathbf{p}(\mathbf{r}_s) = \mathbf{B}_s\mathbf{c} ,$$
(4)

where $\mathbf{B}_s$ denotes the matrix with the elementary wave functions in the reconstruction plane z_s. From the inversion of eq. (3), the coefficients are determined. It follows that the pressure in the reconstruction plane can be estimated as:

$$\mathbf{p}(\mathbf{r}_s) = \mathbf{B}_s\mathbf{B}^+\mathbf{p}(\mathbf{r}_h) ,$$
(5)

where the superscript $^+$ denotes the regularized pseudo-inverse, i.e: $\mathbf{B}^+ = (\mathbf{B}^H\mathbf{B} + \varepsilon\mathbf{I})^{-1}\mathbf{B}^H$, with $\mathbf{I}$ the identity matrix and ε the regularization parameter.

Nevertheless, if we are only interested in the fraction of the flow of energy that propagates into the far field, the evanescent waves must be discarded in the reconstruction to get rid of the near-field circulating energy. An alternative set of elementary waves is thereby defined as

$$\psi_n^{(s)}(\mathbf{r}) = \begin{cases} e^{-j(k_{x,n}x + k_{y,n}y + k_{z,n}(z-z^+))} & \text{if } k^2 \geq k_x^2 + k_y^2 \\ 0 & \text{if } k^2 < k_x^2 + k_y^2 \end{cases} \tag{6}$$

Based on these propagating wave functions, a reconstruction matrix $\mathbf{B}_s^{(s)}$ is defined. It follows that the pressure that propagates to the far field is

$$\mathbf{p}^{(s)}(\mathbf{r}_s) = \mathbf{B}_s^{(s)}\mathbf{B}^+\mathbf{p}(\mathbf{r}_h) . \tag{7}$$

Making use of Euler's equation of motion, the normal component of the particle velocity that propagates to the far field can be estimated as

$$\mathbf{u}_z^{(s)}(\mathbf{r}_s) = \mathbf{B}_s^{(s)}\frac{\mathbf{K}_z^{(s)}}{\rho_0 ck}\mathbf{B}^+\mathbf{p}(\mathbf{r}_h) , \tag{8}$$

where $\mathbf{K}_z^{(s)}$ is a diagonal matrix with the k_z corresponding to each elementary wave of $\mathbf{B}_s^{(s)}$.

The reconstruction can as well be based on the measurement of the particle velocity [8]. In this case the reconstruction equations are:

$$\mathbf{u}_z^{(s)}(\mathbf{r}_s) = \mathbf{B}_s^{(s)}\mathbf{B}^+\mathbf{u}_z(\mathbf{r}_h) , \tag{9}$$

$$\mathbf{p}^{(s)}(\mathbf{r}_s) = \mathbf{B}_s^{(s)}\rho_0 ck\mathbf{K}_z^{(s)-1}\mathbf{B}^+\mathbf{u}_z(\mathbf{r}_h) . \tag{10}$$

Once the propagating part of the pressure and particle velocity have been calculated, the effective sound intensity can be obtained as

$$\mathbf{I}^{(s)}(\mathbf{r}) = \frac{1}{2}\text{Re}\{p^{(s)}(\mathbf{r})\mathbf{u}^{(s)}(\mathbf{r})^*\} , \tag{11}$$

with the superscript * denoting the complex conjugate.

3. NUMERICAL RESULTS

In this section, the calculation of the effective or supersonic intensity with SONAH is examined based on simulated measurements. The results are compared for benchmarking to the existing FFT based methodology [5]. Additionally, the reconstruction based on measurement of sound pressure, particle velocity and a combined measurement of pressure and velocity is examined.

The source used in the experiment was a baffled point source located at the origin of coordinates. The hologram plane was $z = 10$ cm, which served also as the reconstruction plane. The measurement grid consisted of 15 x 15 positions, over an aperture of 60 x 60 cm. The virtual source plane used to scale the plane waves was retracted half an inter-spacing distance behind the reconstruction plane and the wavenumber resolution used was $\Delta k_{(x,y)} = 0.3$. Noise of 35 dB signal-to-noise ratio was added to the simulated measurements.

The effective sound intensity is a quantity that cannot be measured directly, and seldom can it be known analytically. It is however possible to determine it for point sources. Thus, it can be used for assessing the accuracy of a given methodology. The reconstruction error was calculated as:

$$Error[\%] = 100 \cdot ||I^{(s)} - I_{true}^{(s)}|| / ||I_{true}^{(s)}||.$$

The true field of the baffled point source $I_{true}^{(s)}$ was calculated following similar derivations as in ref. [5], but without assuming $z=0$. Numerical integration was therefore required to evaluate the true field. An adaptive recursive Simpson's rule was used, with an error below 10^{-6}.

Figure 1 (a) shows the calculation error based on measurement of the sound pressure with the SONAH method and the FFT based one. SONAH is somewhat more accurate, especially at low frequencies, where the wavelength is comparable to or larger than the measurement aperture. However, at higher frequencies, as the measurement aperture becomes larger in comparison to the wavelength, the truncation error due to the finite aperture decreases, and the accuracy of the two methods is similar.
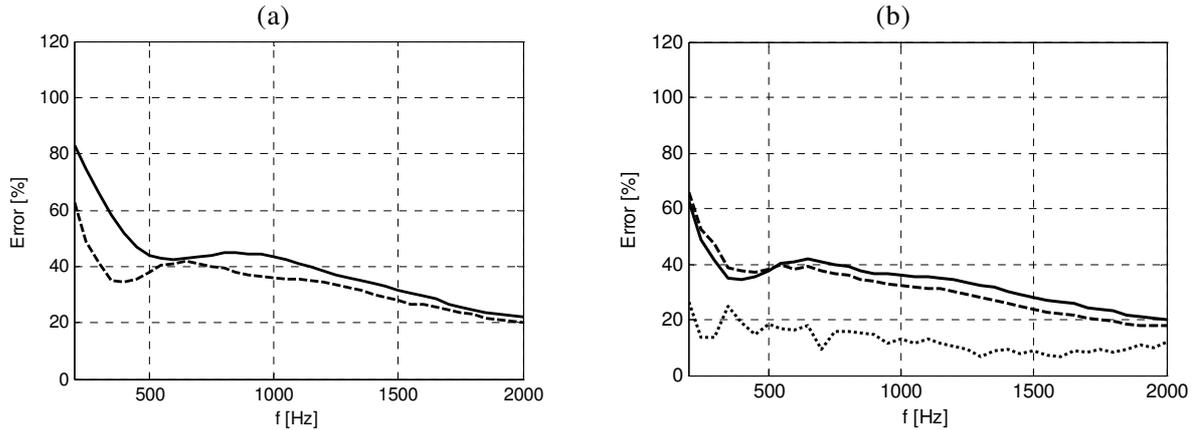
Figure 1 - (a) Calculation error of the effective intensity of a point source using the Fourier based NAH method (solid line), and the SONAH method (dashed line); (b) Calculation error of the effective intensity of a point source with SONAH based on pressure (solid line), on particle velocity (dotted line) and on combined pressure-velocity measurements (dashed line).

Figure 1 (b) shows the calculation error with SONAH based on the measurement of the velocity, the pressure and a combined measurement of sound pressure and particle velocity. The velocity based calculation is consistently better than the pressure or velocity-and-pressure based ones. This is an interesting result, which can be as well explained by the lower truncation error (this will be discussed further in the following, see section 5). At high frequencies, above 1500 Hz, the accuracy of the pressure based calculation improves and is comparable to the velocity based one. The fluctuations of the velocity based reconstruction error are a result of the singularity in the velocity-to-pressure transformation due to the k/k_z ratio in eq. (10), when $k_z=0$.

4. EXPERIMENTAL RESULTS

An experimental study was conducted to study the method proposed and examine further the concept and implications of the effective sound intensity. The measurements took place at the LVA, INSA-Lyon, France. The source used was a steel plate, mounted on a rigid wall of a semi-anechoic chamber. The plate was centered in the origin of coordinates and it was of dimensions (49 x 69) cm and 1 mm thick. It was driven at (7,-15) cm with random noise excitation from 100 Hz to 2500 Hz, and 3 s long Hanning windows for the analysis. The plate was measured at 10 cm distance with a line array of 11 p-u probes (see Figure 2). A grid of 11 x 16 positions was measured, over an aperture of 60 x 90 cm. The measured particle velocity was used for the calculation.
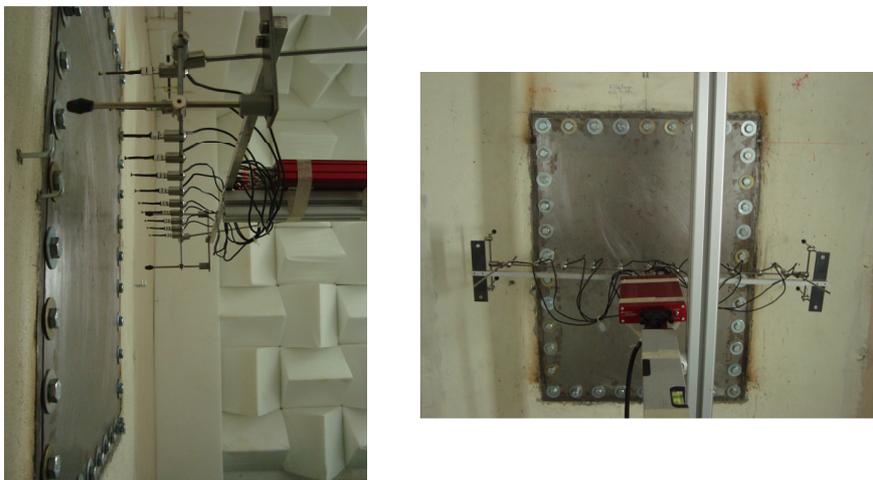

Figure 2 – Experimental set-up: Baffled plate in a semi-anechoic chamber and line array.

Figure 3 and 4 show the measured velocity, the active sound intensity and the effective intensity at 158 Hz and 1 kHz respectively. At 158 Hz (Figure 3), the plate is vibrating in a (1,4) mode-like shape. The measured velocity at 10 cm indicates that the structural wavelength is much smaller than the wavelength in air, creating a highly reactive field with a strong circulatory flow of energy. This is reflected in the active sound intensity map, which shows how there are two regions of the pate that act as 'sinks' of energy, with negative sound intensity, as opposed to the adjacent regions, that have a positive intensity. Note also that the effective intensity level in this case is one order of magnitude less than the active sound intensity, and its maximum level is found at the driving point.
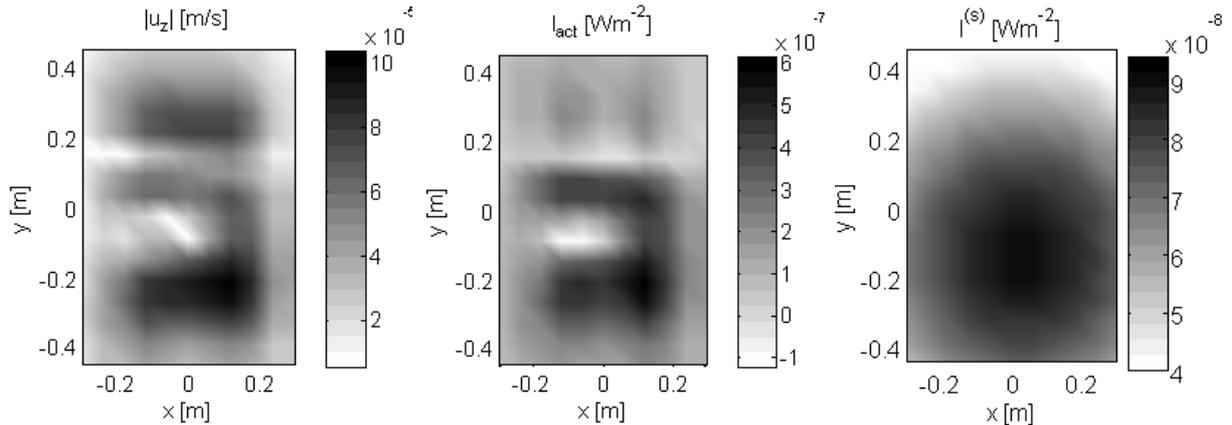
Figure 3 – Measured normal velocity (left), calculated active intensity (centre) and effective intensity (right) at frequency f=158 Hz. All quantities at 10 cm from the plate.

Figure 4 shows the same quantities at 1 kHz. Note that at this frequency, the structural wavelength is approximately 10 cm, and the evanescent waves radiated by the source have decayed significantly at the measurement plane. Therefore, the propagating waves dominate, and as a result, the active intensity and the effective intensity are nearly identical, since there is no circulatory energy in the measurement plane. This result validates the consideration that the effective intensity and the active intensity essentially differ by the circulatory flow of energy being removed or not.

Figure 5 shows the active and the effective sound intensity, as in Figures 4 and 5, but plotted through a vertical line at x= -12 cm. In this plot, the intensity levels can be understood more clearly.
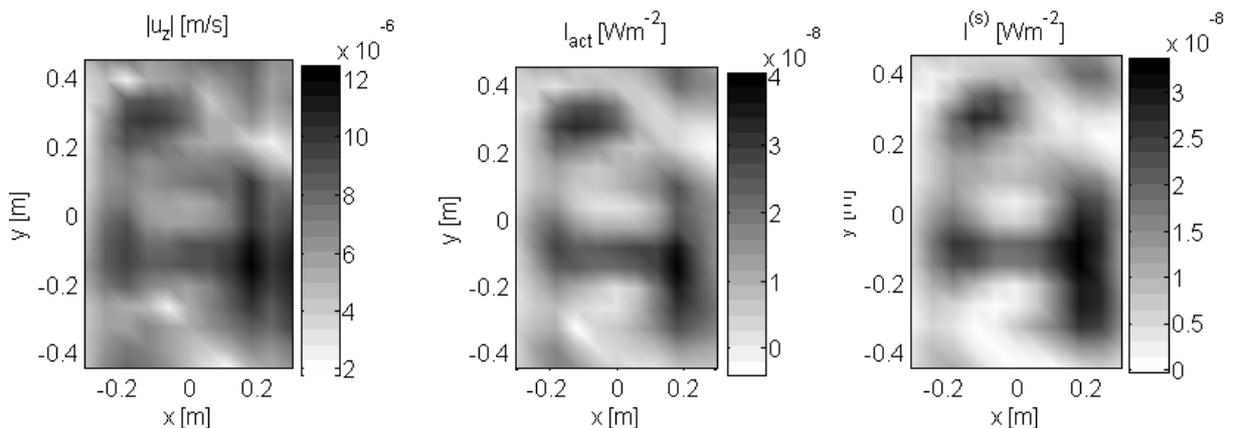
Figure 4 – Measured normal velocity (left), calculated active intensity (centre) and effective intensity (right) at frequency f=1000 Hz. All quantities at 10 cm from the plate.
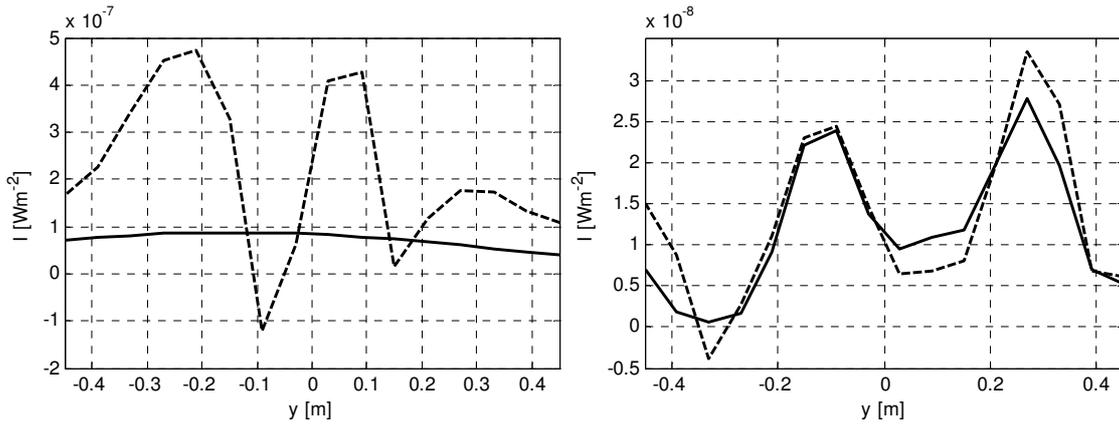
Figure 5 – Active intensity (dashed line) and effective intensity (solid line) at frequency f=160 Hz (left) and at 1000 Hz (right) through a vertical line at *x*=-12 cm of the measurement grid.

5. DISCUSSION

One of the strengths of statistically optimized near-field acoustic holography is that it is a patch method that overcomes some of the errors associated with the discrete Fourier transform by directly operating in the spatial domain. It is therefore not surprising that the effective sound intensity calculated with SONAH is more accurate than when it is calculated with conventional FFT based NAH. However, the results of the latter method could be improved by artificially extending the measurement aperture by means of extrapolation [9], making it suitable for patch-NAH.

The results of the investigation show that there is an important error associated with the estimation of the effective intensity, reflected in the high calculation errors of the methods as shown in section 3. This is presumably a natural consequence of the sharp separation between the effective and ineffective radiation, namely, the waves inside and outside the radiation circle (see eq. 6). This is an ideal separation of the wavenumber spectrum in which a "brick-wall" filter is implicitly used. Such a filter has an infinite impulse response in space domain that is much larger than the measurement aperture used in practice. This explains the large relative error of the numerical experiments. Note that this error is not a consequence of the sharp transition between the measured data inside the aperture and the "zeroes" outside, but a consequence of not measuring over an infinite aperture.

This last consideration explains as well why the velocity based calculation is notably more accurate than the other methods, namely because the normal component of the particle velocity decays much faster than the pressure towards the edge of the aperture. When measuring the normal velocity sufficiently close to the source, the measurement aperture could be regarded as virtually infinite, because the normal component of the particle velocity is zero outside of it. Contrarily, this is not the case with the sound pressure. This explains why the calculation based on measurement of the particle velocity is more accurate than the one based on combined measurement of pressure and velocity, a result that at first might seem surprising.

6. CONCLUSIONS

This study has examined the concept of effective sound intensity, or supersonic acoustic intensity, based on the statistically optimized near-field acoustic holography method (SONAH), as well as the possibility of basing the reconstruction on measurement of the particle velocity. The study indicates that the calculation based on particle velocity measurements is the most accurate. The SONAH based method provides a somewhat more accurate calculation than the existing methodology. Additionally, an experimental study served to validate the method and verify the relationship between the conventional active intensity and the effective sound intensity.

REFERENCES

[1] F. Fahy, "Sound Intensity" (Elsevier Science Publishers Ltd, Barking, Essex, 1989).
[2] J D Maynard, E. G Williams, and Y. Lee, "Nearfield acoustic Holography I: Theory of generalized holography and the development of NAH," J. Acoust. Soc. Am, 78(4):1395–1413 (1985).

[3] E. G. Williams, "Fourier Acoustics. Sound Radiation and Nearfield acoustic Holography" (Academic Press, San Diego, 1999).

[4] E. G. Williams, "Supersonic acoustic intensity," J. Acoust. Soc. Am., 97(1):121–127 (1994).

[5] E. G. Williams, "Supersonic acoustic intensity on planar sources," J. Acoust. Soc. Am., 104(5), 2845–2850 (1998).

[6] J. Hald, "Basic theory and properties of statistically optimized near-field acoustical holography," J. Acoust. Soc. Am, 125(4): 2105–2120 (2009).

[7] R. Steiner and J. Hald, "Near-field Acoustical Holography Without the Errors and Limitations Caused by the Use of Spatial DFT," International Journal of Acoustics and Vibration, 6(2) (2001).

[8] F. Jacobsen and V. Jaud, "Statistically optimized near field acoustic holography using an array of pressure-velocity probes," J. Acoust. Soc. Am., 121(3):1550–1558 (2007)

[9] E.G. Williams, "Continuation of acoustic near-fields," J. Acoust. Soc. Am. 113(3) , 1273–1281 (2003).